Biophysical characterization of the fusogenic region of HCV envelope glycoprotein E1

Ana J. Pérez-Berná [a], Georg Pabst [b], Peter Laggner [b], José Villalaín [a,*]

[a] Instituto de Biología Molecular y Celular, Universidad "Miguel Hernández", E-03202 Alicante, Spain
[b] Institute of Biophysics and Nanosystems Research, Austrian Academy of Sciences, Graz, Austria

ARTICLE INFO

ABSTRACT

We have studied the binding and interaction of the peptide $E1_{FP}$ with various model membranes. $E1_{FP}$ is derived from the amino acid segment 274–291 of the hepatitis C virus envelope glycoprotein E1, which was previously proposed to host the peptide responsible for fusion to target membranes. In the present study we addressed the changes which take place upon $E1_{FP}$ binding in both the peptide and the phospholipid bilayer, respectively, through a series of complementary experiments. We show that peptide $E1_{FP}$ binds to and interacts with phospholipid model membranes, modulates the polymorphic phase behavior of membrane phospholipids, is localized in a shallow position in the membrane and interacts preferentially with cholesterol. The capability of modifying the biophysical properties of model membranes supports its role in HCV-mediated membrane fusion and suggests that the mechanism of membrane fusion elicited by class I and II fusion proteins might be similar.

© 2009 Elsevier B.V. All rights reserved.

1. Introduction

Hepatitis C virus (HCV) is a small, enveloped positive single-stranded RNA virus that belongs to the genus *Hepacivirus* in the family *Flaviviridae*. HCV is an important public health problem since it is the leading cause of acute and chronic liver disease in humans [1–3]. The HCV genome shows a remarkable sequence variation since more than 90 genotypes distributed into six main types and subtypes have been identified [2]. There is no vaccine to prevent HCV infection, and current therapeutic agents, apart from being associated to different adverse effects, have limited success against HCV [4].

The HCV genome consists of one translational open reading frame encoding a polyprotein precursor which is processed to yield different structural and non-structural proteins [5]. HCV entry into the cell is achieved by the fusion of viral and cellular membranes. Morphogenesis and budding has been suggested to take place in the endoplasmic reticulum [6]. The HCV membrane fusion process is pH-dependent, and low endosomal pH promotes the arrangement of the HCV E1/E2 glycoproteins to its active form [7]. The variability of the HCV proteins gives the virus the ability to escape the host's immune surveillance system and the development of a vaccine is a difficult task [8]. Finding protein–membrane and protein–protein interaction inhibitors could be a good strategy against HCV infection since they might prove to be potential therapeutic agents.

The envelope transmembrane glycoproteins E1 and E2 are anchored to the host cell-derived double-layer lipid envelope. They are essential for entry, binding to receptors and induce fusion with the host-cell membrane as well as in viral particle assembly [9]. These proteins interact with each other and assemble as non-covalent heterodimers; their transmembrane domains (TM) play a major role in heterodimer formation, membrane anchoring and endoplasmic reticulum retention [10]. Studies with HCV_{pp} bearing functional E1 and E2 glycoproteins have probed that HCV viral fusion is dependent on the presence of both E1 and E2 glycoproteins [11]. The presence of cholesterol in target membranes facilitates, but is not essential for, HCV_{pp}-mediated fusion [11]. E1 and E2 are class II fusion proteins with the putative fusion peptide/peptides which is/are supposedly localized in an internal sequence linked by antiparallel β-sheets [12,13]. Many aspects regarding the function and properties of both HCV E1 and E2 glycoproteins still remain unresolved; even so, the location of the fusion peptide is controversial since several data suggest that it could be located in either E1 or E2 or both [7,11,14–16].

Recently, we have identified the membrane-active regions of the HCV E1, E2, core and p7 proteins by studying the effect of protein-derived peptide libraries on model membrane integrity [17–19]. These results indicate the possible location of different segments in these proteins which might be implicated in protein–lipid and protein–protein interactions, helping us to understand the mechanisms that underlay the interaction between viral proteins and membranes. Proteomics computational tools located the fusion peptide in the E1 region comprised by amino acids 272 to 281. This region contains cysteine residues and a core of aromatic and hydrophobic residues [12]. Peptides derived from this region have significant experimental membranotropic leakage, hemifusion and fusion effects [19] (see Fig. 1). Membrane fusion is a complex process that involves several regions of the fusion proteins. The fusion proteins must bring the viral and cellular membranes together, create membrane defects, induce hemifusion and fusion, and form pores within the membranes [20–22]. In order to elucidate the nature of the interaction between phospholipids and membrane proteins and in particular to understand the structural function of the fusion peptide in E1 HCV, we have characterized the interaction of $E1_{FP}$, a peptide derived from the amino acid sequence 274–291 of the HCV E1 glycoprotein fusion domain, with model membranes using biophysical techniques. We demonstrate that the $E1_{FP}$ peptide strongly partitions into phospholipid membranes, locates in a shallow position in the membrane, increases the dipole membrane potential, and leads to lipid mixing depending on the cholesterol concentration in the membrane. Furthermore, $E1_{FP}$ increases membrane disorder and stabilizes the presence of non-lamellar structures, without changing the membrane thickness significantly. Thus, our study provides new evidence for the functional role of this region in the membrane fusion mechanism of HCV.

2. Materials and methods

2.1. Materials and reagents

The peptide $E1_{FP}$ corresponding to the sequence [274]AMYVGDLCG-SIFLVSQLFT[291] from HCV strain 1B4J (with N-terminal acetylation and C-terminal amidation) was obtained from Genemed Synthesis, San Antonio, Texas. The peptide $E1_{FP}$ was purified by reverse-phase HPLC (Vydac C-8 column, 250×4.6 mm, flow rate 1 ml/min, solvent A, 0.1% trifluoroacetic acid, solvent B, 99.9 acetonitrile and 0.1% trifluoroacetic acid) to better than 95% purity, and its composition and molecular mass were confirmed by amino acid analysis and mass spectroscopy. Residual trifluoroacetic acid, used both in peptide synthesis and in the high-performance liquid chromatography mobile phase, was removed by several lyophilisation/solubilisation cycles in 10 mM HCl [23]. Egg L-α-phosphatidylcholine (EPC), egg L-α-phosphatidic acid (EPA), egg sphingomyelin (ESM), bovine brain phosphatidylserine (BPS), egg L-α-phosphatidylglycerol (EPG), cholesterol (CHOL), liver lipid extract (LV), 1,2-dielaidoyl-sn-glycero-3-phosphoethanolamine (DEPE), and 1-palmitoyl-2-oleoyl-sn-glycero-3-phosphocholine (POPC) were obtained from Avanti Polar Lipids (Alabaster, AL, USA). Lissamine rhodamine B 1,2-dihexadecanoyl-sn-glycero-3-phosphoethanolamine (N-RhB-PE), N-(7-nitrobenz-2-oxa-1,3-diazol-4-yl)-1,2-dihexadecanoyl-sn-glycero-3-phosphoethanolamine (NBD-PE), fluorescein-phosphatidylethanolamine (FPE) and 4-(2-(6-(Dioctylamino)-2-naphthalenyl) (ethenyl)-1-(3-sulfopropyl)-pyridinium inner salt (di-8-ANEPPS) were obtained from Molecular Probes (Eugene, OR). 5-Carboxyfluorescein (CF), (>95% by HPLC), 5-doxyl-stearic acid (5NS), 16-doxyl-stearic acid (16NS), dehydroergosterol (ergosta-5,7,9(11),22-tetraen-3ß-ol, DHE), sodium dithionite, deuterium oxide (99.9% by atom), Triton X-100, EDTA, and HEPES were purchased from Sigma-Aldrich (Madrid, ES). All other
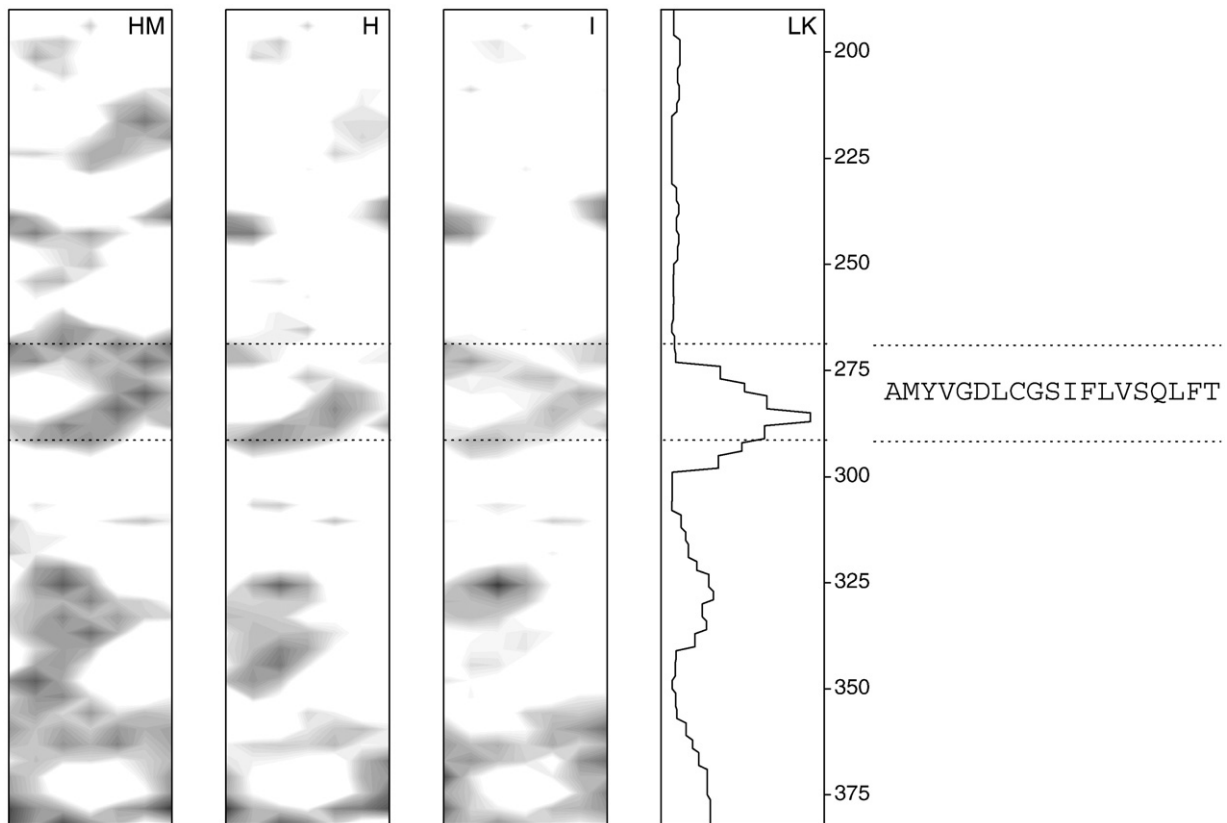
Fig. 1. Hydrophobic moment (HM), hydrophobicity (H), and interfacial hydrophobicity (I) distribution, for HCV E1 envelope glycoprotein [19] assuming that it forms an α-helical wheel [71]. Only positive bilayer-to-water transfer free-energy values are shown (the darker, the greater). A summary of the normalized experimental membrane rupture data (LK) corresponding to 18-mer peptide libraries derived from the whole HCV E1 [19] protein is also shown, as well as the sequence and the location of the $E1_{FP}$ peptide.

reagents used were of analytical grade from Sigma-Aldrich (Madrid, EU). Water was deionized, twice-distilled and passed through a Milli-Q equipment (Millipore Ibérica, Madrid, ES, EU) to a resistivity better than 18 MΩ cm.

2.2. Vesicle preparation

Aliquots containing the appropriate amount of lipid in chloroform/methanol (2:1, v/v) were placed in a test tube, the solvents removed by evaporation under a stream of O_2-free nitrogen, and finally, traces of solvents were eliminated under vacuum in the dark for more than 3 h. The lipid films were resuspended in an appropriate buffer and incubated either at 25 °C or 10 °C above the phase transition temperature (T_m) with intermittent vortexing for 30 min to hydrate the samples and obtain multilamellar vesicles (MLV). The samples were frozen and thawed five times to ensure complete homogenization and maximization of peptide/lipid contacts with occasional vortexing. Large unilamellar vesicles (LUV) with a mean diameter of 0.1 and 0.2 μm for either leakage or lipid mixing and fusion experiments were prepared from multilamellar vesicles by the extrusion method [24] using polycarbonate filters with a pore size of 0.1 and 0.2 μm (Nuclepore Corp., Cambridge, CA, USA). The phospholipid and peptide concentration were measured by methods described previously [25,26].

2.3. Membrane leakage measurement

LUVs with a mean diameter of 0.1 μm were prepared as indicated above in buffer containing 10 mM Tris, 20 mM NaCl, pH 7.4, and CF at a concentration of 40 mM. Non-encapsulated CF was separated from the vesicle suspension through a Sephadex G-75 filtration column (Pharmacia, Uppsala, SW, EU) eluted with buffer containing 10 mM TRIS, 100 mM NaCl, 1 mM EDTA, pH 7.4. Membrane rupture (leakage) of intraliposomal CF was assayed by treating the probe-loaded liposomes (final lipid concentration, 0.125 mM) with the appropriate amounts of peptide using a 5 × 5 mm fluorescence cuvette on a Varian Cary Eclipse spectrofluorometer , stabilized at 25 °C with the appropriate amounts of peptide, each cuvette containing a final volume of 400 μl. The medium in the cuvettes was continuously stirred to allow the rapid mixing of peptide and vesicles. Leakage was assayed until no more change in fluorescence was obtained. The fluorescence was measured using a Varian Cary Eclipse spectrofluorometer. Changes in fluorescence intensity were recorded with excitation and emission wavelengths set at 492 and 517 nm, respectively. Excitation and emission slits were set at 5 nm. One hundred percent release was achieved by adding Triton X-100 to the cuvette to a final concentration of 0.5% (w/w). Fluorescence measurements were made initially with probe-loaded liposomes, afterwards by adding peptide solution and finally by adding Triton X-100 to obtain 100% leakage. Leakage was quantified on a percentage basis according to the equation $\%L = [(F_f - F_0)^* 100] / (F_{100} - F_0)$, where F_f is the equilibrium value of fluorescence after peptide addition, F_0 is the initial fluorescence of the vesicle suspension, and F_{100} is the fluorescence value after the addition of Triton X-100.

2.4. Phospholipid-mixing measurement

Peptide-induced vesicle lipid mixing was measured by resonance energy transfer [27]. This assay is based on the decrease in resonance energy transfer between two probes (NBD-PE and RhB-PE) when the lipids of the probe-containing vesicles are allowed to mix with lipids from vesicles lacking the probes. If both types of vesicles fuse in the presence of the peptide, the surface density of the acceptor is reduced, resulting in a decreased efficiency of resonance energy transfer which is measured experimentally. These changes in transfer efficiency allow quantitative measurements of the lipid-mixing process [31]. The concentration of each of the fluorescent probes within the liposome membrane was 0.6 mol%. LUVs with a mean diameter of 0.2 μm were

prepared as described above. Labeled and unlabeled vesicles in a proportion 1:4 were placed in a 5 mm × 5 mm fluorescence cuvette at a final lipid concentration of 100 μM in a final volume of 400 μl, stabilized at 25 °C under constant stirring. The fluorescence was measured using a Varian Cary Eclipse fluorescence spectrometer using 467 nm and 530 nm for excitation and emission, respectively. Excitation and emission slits were set at 10 nm. Since labeled and unlabeled vesicles were mixed in a proportion of 1 to 4 respectively, 100% phospholipid mixing was estimated with a liposome preparation in which the membrane concentration of each probe was 0.12% [28]. Phospholipid mixing was quantified on a percentage basis according to the equation % PM = ($(F_f - F_0) / (F_{100} - F_0)$] · 100, F_f being the value of fluorescence obtained 15 min after peptide addition to a liposome mixture containing liposomes having 0.6% of each probe plus liposomes without any fluorescent probe, F_0 the initial fluorescence of the vesicles and F_{100} as the fluorescence value of the liposomes containing 0.12% of each probe. It should be taken into account that the characteristic lipid flip-flop time is much longer than the lipid-mixing measurement time.

2.5. Inner-monolayer phospholipid-mixing (fusion) measurement

Peptide-induced phospholipid mixing of the inner monolayer was measured by a modification of the resonance energy transfer method described above [31]. LUVs prepared as above were treated with sodium dithionite to completely reduce the NBD-labeled phospholipid located at the outer monolayer of the membrane. Final concentration of sodium dithionite was 100 mM (from a stock solution of 1 M dithionite in 1 M TRIS, pH 10.0) and incubated for approximately 1 h on ice in the dark. Sodium dithionite was then removed by size exclusion chromatography through a Sephadex G-75 filtration column (Pharmacia, Uppsala, Sweden) eluted with buffer containing 10 mM TRIS, 100 mM NaCl, and 1 mM EDTA, pH 7.4. The proportion of labeled and unlabeled vesicles, lipid concentration and other experimental conditions were the same as indicated above for the phospholipid-mixing assay. In order to eliminate any artifact in the measurements, for each membrane composition zero values were obtained using the fluorescent values of inner monolayer-labeled vesicles without peptide whereas 100% fusion was estimated with vesicles containing 0.12% of each probe measured at the same time the samples were incubated with the peptide.

2.6. Peptide binding to vesicles

The partitioning of the peptide into the phospholipid bilayer was monitored by the fluorescence enhancement of tyrosin. Fluorescence spectra were recorded in a SLM Aminco 8000C spectrofluorometer with excitation and emission wavelengths of 274 and 305 nm, respectively, and 4 nm spectral bandwidths. Measurements were carried out in 20 mM HEPES, 50 mM NaCl, and EDTA 0.1 mM, pH 7.4. Intensity values were corrected for dilution, and the scatter contribution was derived from lipid titration of a vesicle blank. Partitioning coefficients were obtained using $I / I_0 = 1 + [(I_{max} / I_0 - 1)^* ((K_P^*[L]) / ([W] + K_P^*[L]))]$, where I and I_0 are the final and the initial intensities respectively, K_P is a mole fraction partition coefficient that represents the amount of peptide in the bilayers as a fraction of the total peptide present in the system, I_{max} is a variable value for the fluorescence enhancement at complete partitioning determined by fitting the equation to the experimental data, $[L]$ is the lipid concentration, and $[W]$ is the concentration of water (55.3 M) [29]. The peptide concentration in the assays was 30 μM.

2.7. Fluorescence quenching of Tyr emission by water-soluble and lipophylic probes

For acrylamide quenching assays, aliquots from a 4 M solution of the water-soluble quencher were added to the solution-containing peptide in the presence and absence of liposomes at a peptide/lipid

molar ratio of 1:50. The results obtained were corrected for dilution and the scatter contribution was derived from acrylamide titration of a vesicle blank. The data were analyzed according to the Stern–Volmer equation [30], $F_0/F = 1 + K_{SV}[Q]$, where F_0 and F represent the fluorescence intensities in the absence and the presence of the quencher [Q], respectively, and K_{SV} is the Stern–Volmer quenching constant, which is a measure of the accessibility of Tyr to acrylamide. Quenching studies with lipophylic probes were performed by successive addition of small amounts of 5NS or 16NS in ethanol to the samples of the peptide incubated with LUV. The final concentration of ethanol was kept below 2.5% (v/v) to avoid any significant bilayer alterations. After each addition an incubation period of 15 min was kept before the measurement. The excitation and emission wavelengths were 274 and 305 nm, respectively. The data were analyzed as previously described [31].

2.8. Fluorescence measurements using FPE-labeled membranes

LUVs with a mean diameter of 0.1 μm were prepared in buffer containing 10 mM TRIS–HCl, pH 7.4. The vesicles were labeled exclusively in the outer bilayer leaflet with FPE as described previously [32]. Briefly, LUVs were incubated with 0.1 mol% FPE dissolved in ethanol (never more than 0.1% of the total aqueous volume) at 37 °C for 1 h in the dark. Any remaining unincorporated FPE was removed by gel filtration on a Sephadex G-25 column equilibrated with the appropriate buffer. FPE-vesicles were stored at 4 °C until use in an oxygen-free atmosphere. Fluorescence time courses of FPE-labeled vesicles were measured after the desired amount of peptide was added into 400 μl of lipid suspensions (200 μM lipid) using a Varian Cary Eclipse fluorescence spectrometer. Excitation and emission wavelengths were set at 490 and 520 nm, respectively, using excitation and emission slits set at 5 nm. Temperature was controlled with a thermostatic bath at 25 °C. The contribution of light scattering to the fluorescence signals was measured in experiments without the dye and was subtracted from the fluorescence traces. The data were analyzed as previously described [28].

2.9. Measurement of the membrane dipole potential using di-8-ANEPPS-labeled membranes

Aliquots containing the appropriate amount of lipid in chloroform–methanol (2:1 v/v) and di-8-ANEPPS were placed in a test tube to obtain a probe/lipid molar ratio of 1:100 and LUVs, with a mean diameter of 90 nm, were prepared as described previously. Steady-state fluorescence measurements were recorded with a Varian Cary Eclipse spectrofluorometer. The excitation ratio, R_{ex}, is defined as the ratio of emission intensity at 620 nm caused by excitation with 450 and 520 nm light [33]. The mechanism by which di-8-ANEPPS operate in order to sense dipole potential is believed to be electrochromic; absorption and emission peaks shift in response to a nearby electrical field that differentially interacts with the ground state and excited state dipole moments of the chromophore [33]. Therefore di-8-ANEPPS can be used as a ratiometric probe of dipole potential but using an excitation ratio [34]. The lipid concentration was 200 μM, and all experiments were performed at 25 °C.

2.10. FRET with DHE

Vesicles contained POPC/ESM/CHOL at a molar ratio of 50:25:25 plus variable proportions of DHE. The ratio of DHE/CHOL was 0, 0.05, 0.1, 0.17, 0.25, 0.42 and 1. The total lipid concentration was 2 mM and the lipid-to-peptide ratio was 50:1. The suspensions containing both peptide and lipid were incubated overnight. Fluorescence spectra were recorded in a SLM Aminco 8000 spectrofluorometer with excitation at 274 for tyrosine and emission of both tyrosine (donor) and DHE (acceptor) were recorded between 290–500 nm. The

experimentally determined values of FRET efficiency, E, were calculated according to [35].

2.11. Small-angle X-ray scattering experiments

MLVs at a concentration of 5% (w/w) prepared without or with the peptide at a lipid/peptide molar ratio of 50:1 were prepared as stated above and submitted to 15 temperature cycles (heating at 45 °C and cooling at −20 °C). Lipid, at a concentration of 67 mM, was resuspended in buffer containing 20 mM HEPES, and 50 mM NaCl, pH 7.4. Small-angle X-ray diffraction (SAXD) measurements were carried out using a Hecus SWAX-camera (Hecus X-ray Systems, Graz, Austria) as described previously [36] using Ni-filtered Cu-Kα radiation ($\lambda = 1542$ Å) originating from a sealed tube X-ray generator (Seifert, Alvenburg, Germany) operating at a power of 2 kW (50 kV, 4 mA). Sample-to-detector distance was 27.8 cm. A linear-position-sensitive detector was used with 1024-channel resolution. SAXD angle calibration was done with silver stearate. The measurements were performed with the sample placed in a thin-walled 1-mm diameter quartz capillary held in a steel cuvette holder at different temperatures with an exposure time of 1 h. The SAXD curves were analyzed after background subtraction and normalization in terms of a full q-range model using the program GAP [37].

2.12. ^{31}P NMR

Samples were prepared as described above at a lipid/peptide molar ratio of 50:1 and concentrated by centrifugation (14,000 rpm for 15 min). ^{31}P NMR spectra were recorded at different temperatures in the Fourier transform mode in a Bruker Avance 500 MHz NMR (Bruker BioSpin) spectrometer operating at a resonance frequency of 202.38 MHz for ^{31}P-nuclei using a 4-mm CP-MAS probe. The samples were packed into 4-mm zirconia rotors and placed in the spinning module of the CP-MAS probe; no spinning and no cross-polarization were used. Probe temperature was maintained by a Bruker BVT 3000 variable digital temperature unit. Measurements, spectra acquisition, and calibration were essentially performed as previously described [38]. MAS ^{31}P NMR spectra were obtained using a Bruker 4-mm CP-MAS probe without cross-polarization. The spinning speed was 9 kHz, regulated to 3 Hz by a Bruker pneumatic unit and the temperature was 25 °C. Measurements, spectra acquisition and calibration were essentially performed as previously described [17]. A single ^{31}P 90° pulse, typically of 4 μs, was used for excitation, a gated broadband decoupling of 10 W, 32 k data points, 1600 transients and 5 s delay time between acquisitions.

2.13. Hydrophobic moment, hydrophobicity and interfacial hydrophobicity

Hydrophobic moment, hydrophobicity and interfacial hydrophobicity values were obtained from [39–41]. Two-dimensional plots of the hydrophobic moments, hydrophobicity and interfacial hydrophobicity have been obtained using a window of seven amino acids, taking into consideration the arrangement of the amino acids in the space assuming an α-helical structure [42]. Positive values represent positive bilayer-to-water transfer free-energy values and therefore, i.e., the higher the value, the greater the probability to interact with the membrane surface and/or the hydrophobic core.

3. Results

The HCV E1 envelope glycoprotein is thought to be responsible for the membrane fusion process whereas the HCV E2 envelope glycoprotein is thought to mediate the binding to the host cell, although other roles could not be ruled out [7,11,43]. Several hydrophobic patches have been identified in both the E1 and E2 proteins which might be important

for modulating membrane binding and interaction [15,19]. In Fig. 1 we present the analysis of the hydrophobic moment, hydrophobicity and interfacial hydrophobicity distribution along the E1 envelope glycoprotein sequence of HCV (strain 1B4J) assuming it forms an α-helical wheel along the whole sequence [19]. This analysis renders the potential surface zones that could be implicated in the modulation of membrane binding and/or protein interaction. As depicted in Fig. 1, the sequence comprising residues 274–291 is one of the most membranotropic regions of HCV E1 [19] and probably this segment participates in the viral fusion process [11]. For this reason we studied the interaction of E1$_{FP}$, a peptide which comprises the residues 274–291 of this region, with model membranes. In particular, we have focused on the binding and interaction of E1$_{FP}$ with lipid bilayers, the changes induced in both the peptide and phospholipid molecules upon membrane binding, as well as the ability to modulate membrane polymorphism. Since we have previously shown that peptide 274–291 did not show any significant difference on membrane rupture at either neutral or acidic pH [19], we have performed all the assays at neutral pH.

The interaction of the E1$_{FP}$ peptide with membrane vesicles was followed by the change of the fluorescence emission of the Tyr residue in the presence of model membranes [44]. It is important to note that membrane fusion in HCV pseudo-particles does not require any protein or receptor at the membrane surface. Fusion is additionally enhanced by the presence of CHOL [7,45]. The quantum yield of a Tyr residue of a peptide or protein normally changes when this amino acid is located in a hydrophobic environment such as a phospholipid membrane, typically leading to an increase of the fluorescence emission intensity. In solution, the E1$_{FP}$ peptide exhibited absorption and emission maxima at 274 and 304 nm, respectively. The shape and wavelength maximum of the spectra in solution and in the presence of membranes were similar. However, the intensity increased significantly in the presence of membrane vesicles, indicating that the Tyr residue of the peptide was in a hydrophobic environment (Fig. 2A). In the presence of EPC/CHOL the increase in the intensity was significantly higher than in the presence of vesicles containing either complex lipids such as LV or negatively-charged phospholipid mixtures like BPS/CHOL, EPA/CHOL and EPG/CHOL (all binary lipid compositions had a molar ratio of 5:1) (Fig. 2A). This approach allowed us to obtain the peptide partition coefficient, K_P, which gave values in the range 10^7 for EPC/CHOL containing liposomes and in the range 10^5 for the other ones. These K_P values are consistent with the tenet that the peptide binds with high affinity to the membrane surface [38,44,46,47].

We have also used the electrostatic surface potential probe FPE [48] to analyze the binding of the E1$_{FP}$ peptide to model membranes (Fig. 2B). As observed in the figure, E1$_{FP}$ had a higher affinity for model membranes containing LV and the system BPS/CHOL, i.e., the smallest dissociation constant was found in the presence of these vesicles. In contrast, the lower affinity was found for the system EPG/CHOL. Being both BPS and EPG negatively-charged phospholipids, it is interesting to note that phosphatidylserine is the most abundant negatively-charged phospholipid in the viral and host-cell membranes and is further involved in lamellar to non-lamellar transitions [49]. In all cases the data could be adjusted to a binding profile having either a sigmoidal (Hill coefficient of approximately 1) or a hyperbolic dependence (data not shown) which might suggest that the interaction of the peptide with the membrane was monomeric.

Fig. 2. (A) Determination of the partition constant, K_P, of E1$_{FP}$ through the change of the intrinsic tyrosine fluorescence in the presence of increasing lipid concentrations, (B) determination of the dissociation constant, K_d, of E1$_{FP}$ through the change of FPE fluorescence in the presence of increasing lipid concentrations and (C) effect of E1$_{FP}$ on the membrane dipole potential monitored through the fluorescence ratio (R_{ex}) of di-8-ANEPPS. LUVs were composed of EPC/CHOL at a molar ratio of 5:1 (○), BPS/CHOL at a molar ratio of 5:1 (◇), EPG/CHOL at a molar ratio of 5:1 (☆), EPA/CHOL at a molar ratio of 5:1 (△) and liver extract lipids (□). Vertical bars indicate standard deviations of the mean of triplicate samples.
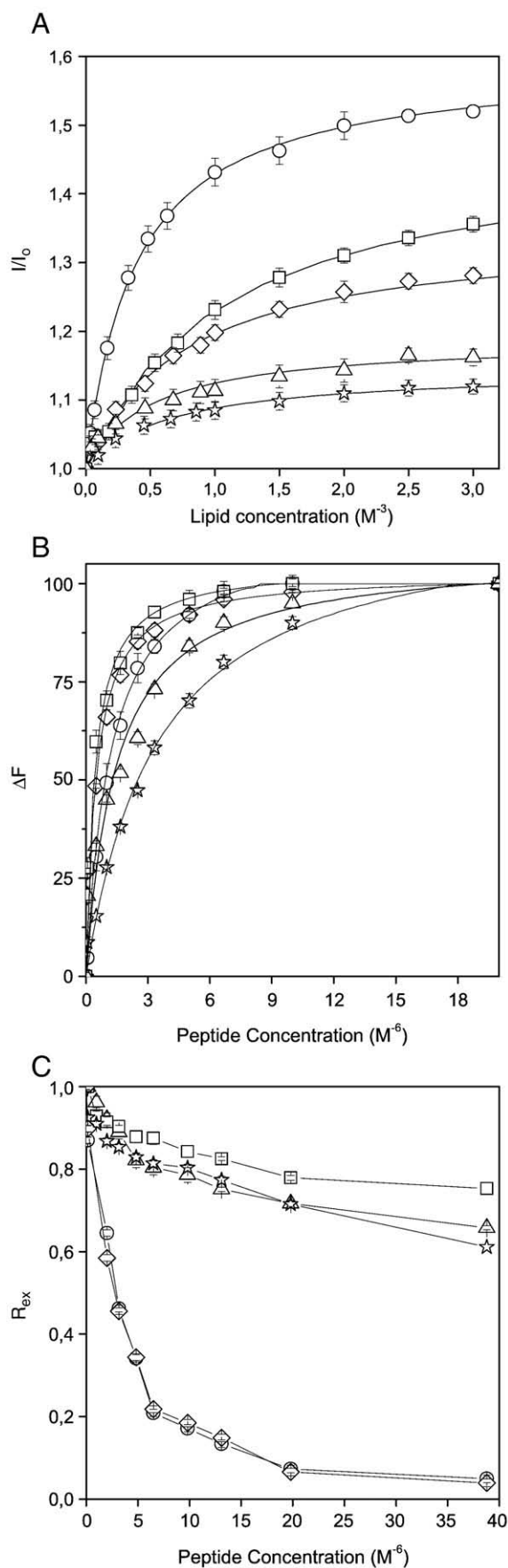
Changes in the magnitude of the membrane dipole potential elicited by $E1_{FP}$ were monitored by the spectral shift of the fluorescence probe di-8-ANEPPS [28]. The variation of the normalized fluorescence intensity ratio $R_{450/520}$ as a function of the peptide concentration for different membrane compositions is shown in Fig. 2C. The data demonstrate that the peptide was capable of inserting into the lipid bilayer, leading to a modification of its dipole potential. The binding of the peptide to the membrane could be described by a saturable binding model where the peptide increased the magnitude of the dipole potential of all the phospholipid bilayers. In the presence of the peptide, the strongest decrease in the $R_{450/520}$ value was obtained in bilayers containing EPC/CHOL and BPS/CHOL.

We also studied the accessibility of the Tyr residue of $E1_{FP}$ towards acrylamide, a neutral, water-soluble, highly efficient quenching molecule, which is unable to penetrate into the hydrophobic core of the lipid bilayer. Stern–Volmer plots for the quenching of Tyr by acrylamide are shown in Fig. 3A. The plots are linear with a unitary intercept showing that the Stern–Volmer dynamic quenching formalism accurately describes the data. In aqueous solution the Tyr residue was highly

exposed to the solvent that led to a more efficient quenching. The lower K_{SV} values obtained in the presence of lipids compared with the higher ones in their absence, suggest that the peptide is buried in the membrane, becoming less accessible for quenching by acrylamide. Interestingly, the K_{SV} values in the presence of EPC/CHOL and LV containing vesicles were greater than in the presence of negatively-charged phospholipids, indicating that the peptide would be located less deeply inside the membrane in the presence of the later phospholipids.

The transverse location of $E1_{FP}$ into the lipid bilayer was evaluated by monitoring the relative quenching of the fluorescence of the Tyr residue by the lipophylic spin probes 5NS and 16NS (Fig. 3B). For 5NS and 16NS, the nitroxide groups are located at about 12 Å and at 3 Å from the bilayer centre [50], so that the direct comparison of the Stern–Volmer plots provides a qualitative method to determine the penetration of the peptide within the bilayer. In general, the peptide was quenched more efficiently by 5NS than by 16NS, suggesting that the peptide remained close to the lipid/water interface. However, the most efficient quenching takes place in membranes composed of EPC/CHOL and LV, indicating that the location of the peptide in the presence of the zwitterionic lipids is deeper than in the presence of negatively-charged phospholipids.

To examine the effect of $E1_{FP}$ in the destabilization of membrane vesicles, we have studied its effect on membrane rupture, i.e., leakage (Fig. 4A). The peptide induced a significant, dose-dependent, leakage effect in all membrane systems studied (at the highest peptide to lipid ratio studied, i.e., 1:5, leakage values were about 95–100%). However, the highest leakage effect was observed for liposomes composed of a LV (Fig. 4A). This data shows that all these membranes are perturbed by the $E1_{FP}$ peptide at all lipid/peptide ratios tested. Membrane perturbation is not sufficient to complete the process of membrane fusion, but also the merging of the monolayers and stalk formation [22]. Therefore, we have also studied the effect of the peptide on both phospholipid mixing and fusion using a probe dilution assay [27,51]. As shown in Fig. 4B and C, the higher phospholipid mixing and fusion values were found for liposomes containing either EPC/CHOL or LV (about 95–100% phospholipid mixing and 80–100% fusion at a peptide to lipid ratio of 1:5), whereas BPS/CHOL, EPG/CHOL and EPA/CHOL displayed lower but also significant values (about 40% phospholipid mixing and 35% fusion at a peptide to lipid ratio of 1:5). Therefore, the lower phospholipid mixing and fusion values were found for liposomes containing negatively-charged phospholipids.

The presence of both sphingomyelin and CHOL has been related to the occurrence of laterally segregated membrane microdomains or "lipid rafts". Interestingly, it has been found for several viruses that there is an important relationship between membrane fusion and the presence of CHOL and sphingomyelin in membranes [52]. In this context, it is further interesting to note that the presence of CHOL has been recently reported to facilitate the fusion of HCV_{pp} with the target membrane [53]. Therefore, we have tested the possibility that CHOL could mediate the interaction of the $E1_{FP}$ peptide with the membrane. Since the energetic barrier for hemifusion is larger than leakage [45], we have chosen lipid mixing to study the possible dependence of $E1_{FP}$ with CHOL. The extent of phospholipid mixing for a number of different POPC/ESM/CHOL compositions at different lipid-to-peptide ratios is shown in Fig. 5A. Significantly, at relatively low lipid/peptide ratios, the higher the CHOL content, the higher the mixing. The dependence of leakage on the molar ratio of each component in the mixture is shown in Fig. 5B. It is readily observed that an increase of the EPC molar ratio leads to a decrease of lipid mixing. In contrast, the content of CHOL correlates directly with an increase of lipid mixing. No pattern can be discerned by changing the molar ratio of ESM (Fig. 5B). These results show that the content of CHOL in the sample is critical for lipid mixing. Probably $E1_{FP}$ interacts specifically with CHOL and/or its effects exerted on membranes depend on its presence. A representation of all studied POPC/ESM/CHOL compositions is shown as a ternary phase diagram in the insert of Fig. 5A. Since this ternary
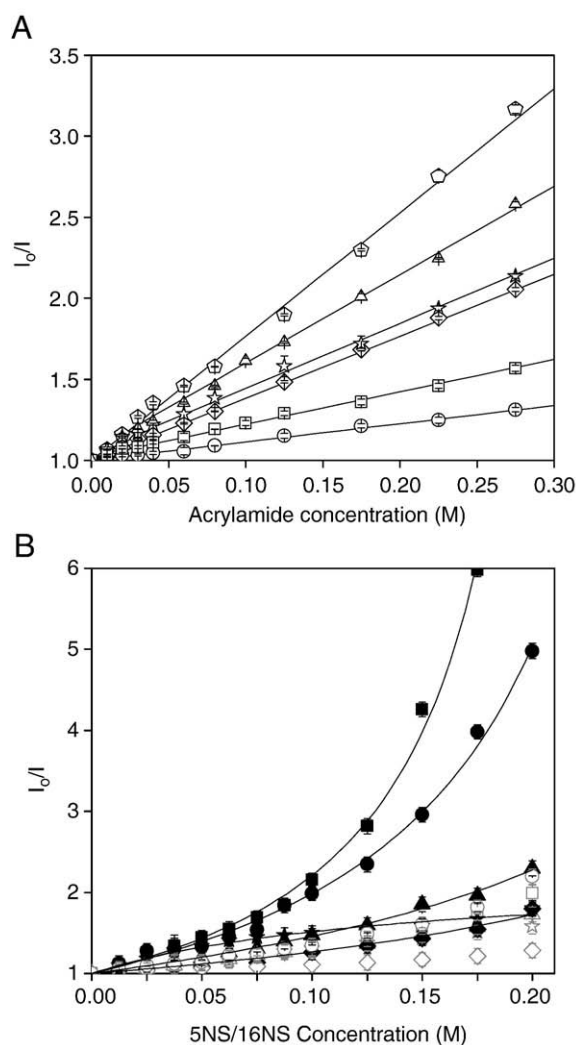

Fig. 3. (A) Stern–Volmer plots of the quenching of the tyrosine fluorescence emission of $E1_{FP}$ by acrylamide and (B) depth-dependent quenching of the tyrosine fluorescence emission of $E1_{FP}$ by 5NS (filled symbols) and 16NS (empty symbols) in LUVs. LUVs were composed of EPC/CHOL at a molar ratio of 5:1 (○,●), BPS/CHOL at a molar ratio of 5:1 (◇,◆), EPG/CHOL at a molar ratio of 5:1 (☆,★), EPA/CHOL at a molar ratio of 5:1 (△,▲) and liver extract lipids (□, ■). Peptide in buffer is represented as (⬡) in (A).
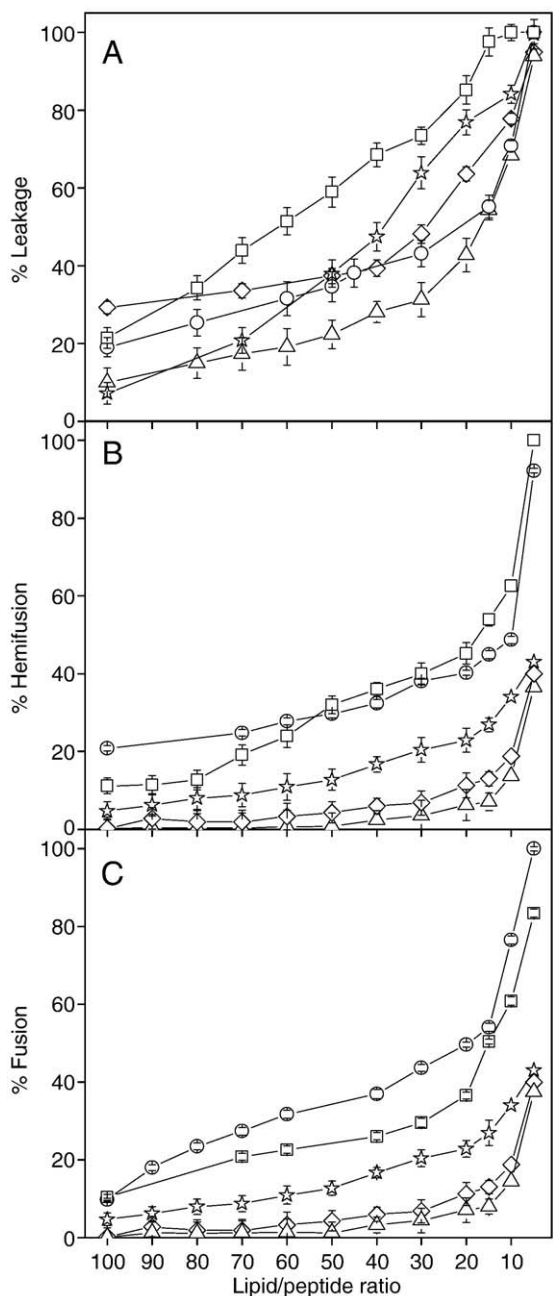
Fig. 4. Effect of E1$_{FP}$ on (A) membrane rupture, i.e., leakage, (B) membrane phospholipid mixing of the outer monolayer, i.e., lipid mixing, and (C) membrane phospholipid mixing of the inner monolayer, i.e., fusion, of fluorescent probes encapsulated in LUVs containing different lipid compositions at different lipid-to-peptide molar ratios. LUVs were composed of EPC/CHOL at a molar ratio of 5:1 (○), BPS/CHOL at a molar ratio of 5:1 (◇), EPG/CHOL at a molar ratio of 5:1 (☆), EPA/CHOL at a molar ratio of 5:1 (△) and liver extract lipids (□).

containing different DHE concentrations. As shown in Fig. 5C, an increase in energy transfer efficiency with increasing DHE concentration, higher than the expected on the basis random distribution, was observed. Therefore, the Tyr residue of the E1$_{FP}$ peptide was in the vicinity of DHE, i.e., adsorption occurred.

Information on the structural organization of a mixture containing POPC/ESM/CHOL at a molar ratio of 5:1:1 in the absence and in the presence of the E1$_{FP}$ peptide was studied by small-angle X-ray diffraction, SAXD (Fig. 6A). This technique defines the macroscopic structure and provides the interlamellar repeat distance in the lamellar phase which comprises both the bilayer and the water layer thickness. The structural results from the global data analysis are shown in the insert of Fig. 6A. Both in the absence and in the presence of the peptide, the diffraction pattern corresponded to the liquid–crystalline L$_\alpha$ phase, showing an interlamellar repeat distance of 67.9 Å for the pure lipid mixture and 70.5 Å in the presence of peptide. The membrane thickness decreased from 43.3 Å in the absence of the peptide to 39.5 Å in its presence. However the thickness of the water layer increased from 24.6 Å to 31.0 Å under the same conditions. Visually, the most significant effect was the increase of the diffuse scattering in the presence of the peptide indicating that several bilayers have become positional uncorrelated due to its influence.

Since the ^{31}P NMR isotropic chemical shifts of both ESM and POPC headgroups are resolvable under MAS NMR conditions, we have used ^{31}P MAS NMR for observing the mixture POPC/ESM/CHOL at a molar ratio of 5:1:1 in the absence and in the presence of the E1$_{FP}$ peptide. As observed in Fig. 6B, the chemical shift for the POPC and ESM resonances was not different neither in the absence nor in the presence of the peptide, but the line widths of the ^{31}P resonances of POPC and ESM were dissimilar. In the absence of the peptide, the ^{31}P line widths at half height were 42.5 Hz and 51 Hz for POPC and ESM respectively, whereas they shifted to 70.4 Hz and 109.9 Hz for POPC and ESM respectively when the peptide was present. These results show that both phospholipids, POPC and ESM, exhibit a lower degree of mobility and/or an increased heterogeneity of headgroup environments in the presence of the peptide. However, ESM showed a higher increase in width at half height than POPC.

Phosphatidylethanolamines in general and DEPE in particular display a gel-to-liquid crystalline phase transition, L$_\beta$–L$_\alpha$, and a lamellar-to-inverted hexagonal phase transition, L$_\alpha$–H$_{II}$. Information on the structural organization of DEPE and DEPE in the presence of peptide was obtained also by SAXD. The diffraction patterns of pure DEPE and DEPE in the presence of the peptide from 25° to 80° are shown in Fig. 7A and B, respectively. Between 25 °C and 60 °C the diffraction patterns of pure DEPE were characteristic of the lamellar phase, whereas at higher temperatures the hexagonal phase was detected. In the presence of the peptide, a coexistence of gel and liquid–crystalline phases was apparent at 35 °C (Fig. 7B). At 60 °C reflections characteristic of the hexagonal phase appeared with a residual refraction of the lamellar phase at higher temperatures (Fig. 7B). Thus, E1$_{FP}$ leads to an increase of both transition widths.

DEPE when organized in bilayer structures gives rise to an asymmetrical ^{31}P NMR line-shape with a high-field peak and a low-field shoulder, presenting a residual chemical shift anisotropy, $\Delta\sigma$, of 36–40 ppm in the gel state and 27–30 ppm in the liquid–crystalline state [55]. In the H$_{II}$ phase the chemical shift anisotropy is further averaged due to rapid lateral diffusion of the phospholipid around the tubes of which this phase is composed, resulting in a line-shape with reverse symmetry, i.e., a high-field shoulder and a low-field peak, accompanied by a twofold reduction in the absolute value of $\Delta\sigma$. This was the behavior we found for pure DEPE as expected (Fig. 7C). However, when E1$_{FP}$ was added to attain a lipid/peptide molar ratio of 50:1, the NMR profile of DEPE was different, since, beginning at approximately 55 °C, an isotropic peak at 0 ppm was apparent, and significantly, a mixture of both lamellar and hexagonal phases was observed at 60 °C, in concordance with the SAXD data shown above (Fig. 7D).

diagram is comparable with that of POPC/PSM/CHOL [54], all samples studied here would have a coexistence of liquid-ordered and liquid-disordered phases, i.e., a high probability of lipid raft domains. It can be also observed that the maximum phospholipid mixing should be obtained at a theoretical lipid composition consisting of about 80% CHOL and about 20% ESM (dotted lines, insert of Fig. 5A). To further confirm the adsorption of E1$_{FP}$ to CHOL in membranes, we have used a fluorescence resonance energy transfer between the fluorescent cholesterol analogue, dehydroergosterol (acceptor) and Tyr (donor) [59] using LUVs of POPC/ESM/(CHOL/DHE) at a molar ratio of 2:1:1
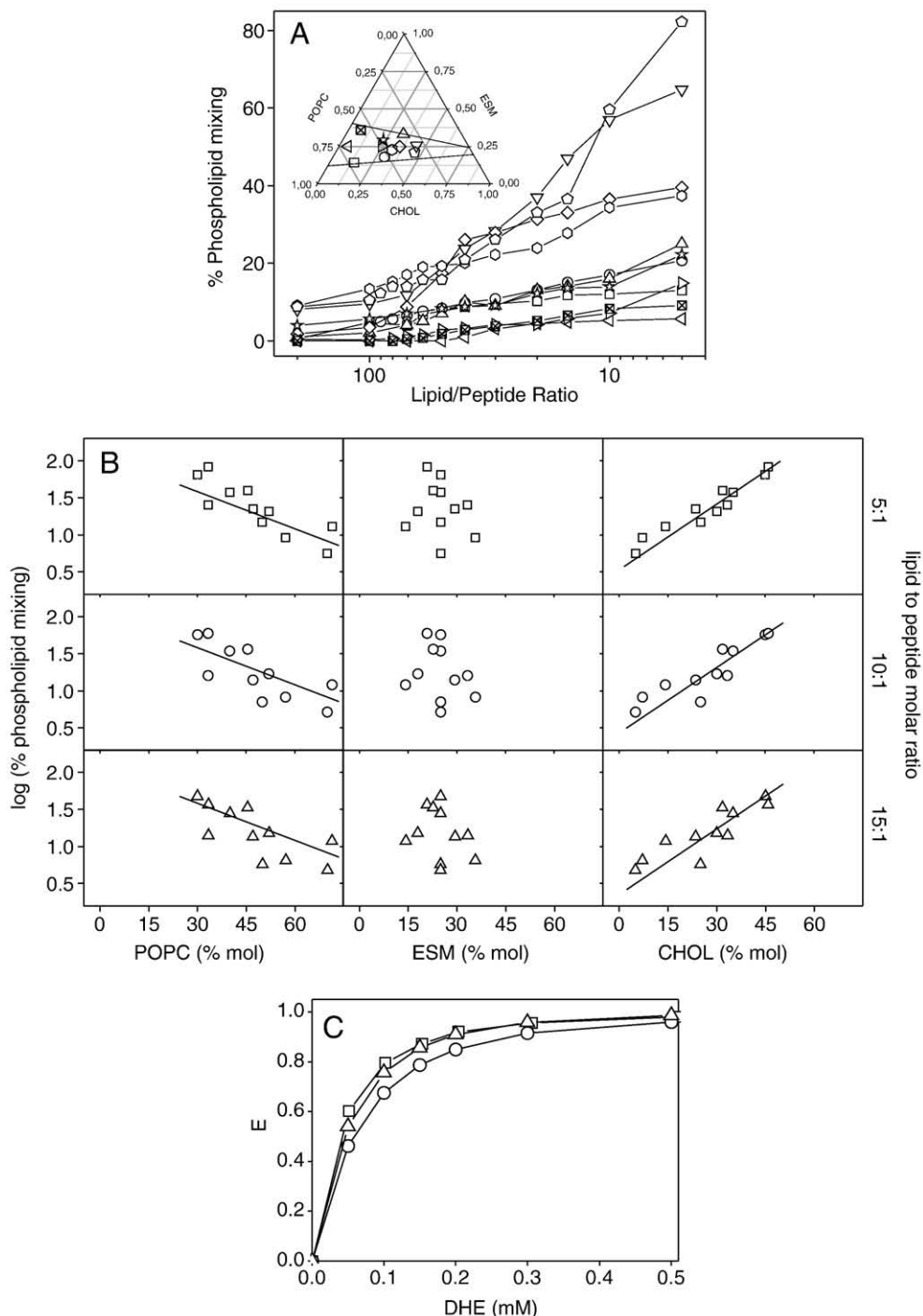
Fig. 5. (A) Effect of E1$_{FP}$ on phospholipid mixing of LUVs composed of POPC/ESM/CHOL at lipid molar ratios of: 14:5:1 (◁), 5:1:1 (□), 2:1:1 (▷), 8:5:1 (⊠), 26:9:15 (○), 8:5:4 (☆), 8:5:7 (◇), 10:5:7 (⬡), 1:1:1 (△), 6:5:9 (▽), and 8:5:11 (⬠). The insert shows the different POPC/ESM/CHOL ratios displayed in a ternary phase diagram. (B) Dependence of phospholipid mixing with the molar percentage of POPC, ESM and CHOL for LUVs composed of POPC/ESM/CHOL at lipid/peptide ratios of 5:1 (□), 10:1 (○) and 15:1 (△). (C) Energy transfer efficiency from the Tyr residue of E1$_{FP}$ to DHE (acceptor) in POPC/ESM/CHOL vesicles at a molar ratio of 2:1:1 (□) and energy transfer efficiency expected for a random distribution using w1 = 10 Å and w2 = 30 Å (○) and w1 = 5 Å and w2 = 25 Å (△) (see ref. [35]).

4. Discussion

Envelope fusion class I and class II glycoproteins, located on the outer surface of the viral membranes, mediate the fusion of the viral and cellular membranes [56,57]. Significantly, class I and class II membrane fusion proteins share structural and functional characteristics in specific domains which interact with and disrupt biological membranes [12,56–58]. It is known that both HCV E1 and E2 envelope glycoproteins are essential for receptor binding, host-cell entry and membrane fusion; however, their specific roles in the different processes of the viral life cycle are not known [9,11,43,59,60]. Moreover, membrane fusion does not necessarily occur at the plasma membrane level; viral entry can also involve endocytosis and vesicular trafficking, as it happens in the case of HCV. The E1/E2 heterodimer is thought to be the functional fusion unit, capable of juxtaposing, destabilizing and merging the viral and cellular membranes so that a fusion-pore is formed. Low-pH would induce its
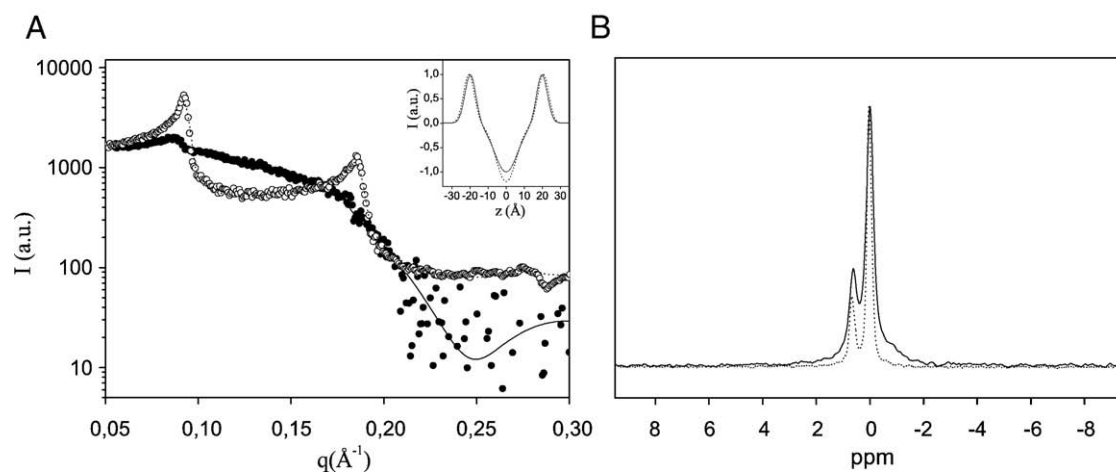
Fig. 6. (A) Small-angle X-ray scattering of an EPC/ESM/CHOL MLV suspension at a molar ratio of 5:1:1 in the absence (○) and in the presence of the E1$_{FP}$ peptide (●). Solid lines represent the best fit to the SAXD data applying a global analysis technique. The insert displays the one dimensional electron density profiles along the bilayer normal calculated from the SAXD diffraction patterns in the absence (····) and in the presence of the peptide (——). Panel (B) shows MAS ^{31}P NMR spectra of an EPC/ESM/CHOL MLV suspension at a molar ratio of 5:1:1 in the absence (····) and in the presence (——) of the E1$_{FP}$ peptide at a phospholipid/peptide molar ratio of 50:1. The ^{31}P NMR spectra have been normalized. Data was obtained at 25 ℃.

dissociation leading to homo-oligomerization of the active form of the fusion protein [11,60–62]. Several hydrophobic segments have been identified in both E1 and E2 envelope glycoproteins which might be important in the mechanism of membrane fusion, not only for modulating membrane binding and interaction, but also for protein–protein interaction [15,16,19,43,63]. These segments bind and destabilize the biological membrane, and these interactions should be decisive for membrane fusion. In this work we have characterized the interaction of E1$_{FP}$, a peptide derived from one of the most membranotropic regions the HCV E1 glycoprotein (amino acids 274–291), with model membranes. This study provides new evidence for the functional role of this region in the membrane fusion mechanism of HCV.

E1$_{FP}$ binds with high affinity to different types of phospholipid model membranes. The main binding force is apparently of hydrophobic origin, most likely due to the high hydrophobicity and interfacial hydrophobicity values shown in the peptide sequence (Fig. 1). After binding, the peptide decreased the dipole potential of the membrane. Even though the Tyr residue is located in the N-terminal part of E1$_{FP}$, we have been able to study the binding of the peptide to membrane vesicles by hydrophilic and lipophilic quenching probes. E1$_{FP}$ was less accessible for quenching by acrylamide in the presence of zwitterionic and complex phospholipids than in the presence of negatively-containing membranes, implying a buried location in the former compositions. Similar results were obtained in the presence of NS probes, since a higher quenching efficiency was observed for model membranes containing zwitterionic and complex phospholipids (i.e., liver lipid extract). Nevertheless, the peptide was capable of binding with high affinity to model membranes containing both negatively-charged and zwitterionic phospholipids and it was located near the membrane lipid/water interface.

E1$_{FP}$ disrupted the membrane causing the release of fluorescent probes. This effect was found to depend on lipid composition and on the lipid/peptide molar ratio. The highest effect was observed for liposomes containing a complex mixture of phospholipids, but lower although significant leakage values were also observed for liposomes composed of zwitterionic and negatively-charged phospholipids. The induction of lipid mixing and fusion by E1$_{FP}$ were also studied and similar results were obtained, since specific and large membrane lipid mixing and fusion values were found in the presence of liposomes composed of complex, negatively-charged and zwitterionic phospholipids. Membrane rupture by E1$_{FP}$ is therefore mainly due to hydrophobic interactions within the bilayer; however, the charge of the phospholipid headgroups also affects to some extent membrane leakage. Interestingly, the presence of CHOL

has recently been described to facilitate the fusion with the target membrane of HCV$_{pp}$ [53]. We demonstrate here that CHOL indeed is one of the major determinants of the effects produced by E1$_{FP}$ on membranes since it specifically interacts with CHOL and its effect depends on the molar ratio of this molecule. Even so, the presence of raft domains could be also decisive for the biological function of the protein region where the E1$_{FP}$ peptide resides.

Moreover, the presence of E1$_{FP}$ decreased membrane thickness and increased its hydration layer and at the same time induced the presence of positionally uncorrelated bilayers. Membrane thinning is a frequently found response of lipid bilayers to binding of peptides [64], but not necessarily a universal behavior [65]. It can be understood as the formation by the surface adsorbed peptide of a local dimple [66] that leads to a global decrease of the bilayer thickness. This effect will lead to an overall decrease of the bending rigidity, which facilitates fusion by reducing the free-energy barriers for passing through highly curved intermediate states [67]. Indeed, the increase of the water layer, as well as the partial loss of positional correlations between adjacent bilayers indicate membrane softening, driving some of the stacked bilayers into an unbound state [68,69]. Additionally, the phosphate groups of the phospholipid molecules displayed a lower degree of mobility and/or an increased heterogeneity of headgroup environments in the presence of E1$_{FP}$. This result strengthens that the location of the peptide is at or near the membrane interface. Interestingly, E1$_{FP}$ changed the polymorphic phase behavior of the membranes, since it induced the presence of an H$_{II}$ phase at slightly lower temperatures than in pure DEPE bilayers.

In conclusion, E1$_{FP}$ was able to affect the elastic and structural properties of lipid bilayers, leading to a significant effect on both membrane fusion and leakage, which also depended upon the concentration of CHOL [53]. These effects are possibly related to the conformational changes which might occur on E1 glycoprotein during the fusion process. As it has been suggested previously, the E1 region where E1$_{FP}$ resides might have an essential role in the membrane fusion process, as it has been observed for other analogous proteins (i.e., HIV gp41). In principle only peptides affecting the lipid polymorphic phase behavior could be located in regions implicated in a stabilization/destabilization role of lamellar/non-lamellar structures, the role needed for membrane fusion. Furthermore, E1$_{FP}$ would interact with the membrane through both electrostatic and hydrophobic effects, leading to an adsorption to the membrane interface. It is known that several fusion peptide fragments are prone to promote the formation of local nipples in the cell membrane leading to the formation of local bends and
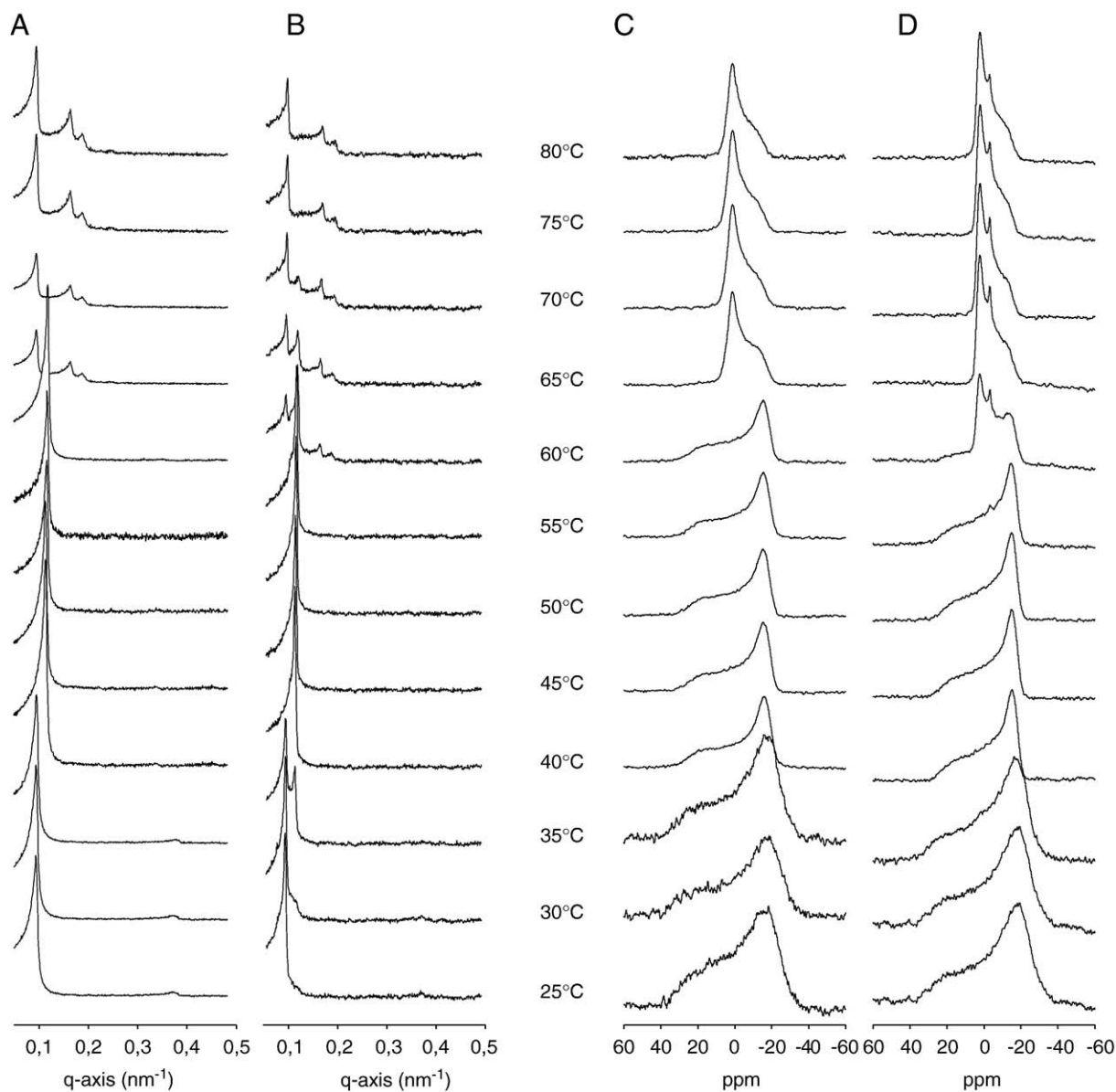
Fig. 7. (A,B) Small-angle X-ray scattering patterns and (C,D) static ^{31}P NMR spectra of DEPE phospholipid dispersions in the absence (A,C) and in the presence (B,D) of the E1$_{FP}$ peptide at a phospholipid/peptide molar ratio of 50:1 at different temperatures as stated. The ^{31}P NMR spectra have been normalized.

therefore non-lamellar phases needed for the fusion process [70]. Therefore, this implies that both HCV E1 and E2 glycoproteins are directly involved in the mechanism that facilitates the entry of the HCV virus into its cellular host. Whereas other membranotropic segments would be implicated in membrane destabilization, pore formation and enlargement, fusion peptides from both E1 and E2 would be of importance in the very first steps of membrane fusion.

Acknowledgements

References

[1] S.L. Chen, T.R. Morgan, The natural history of hepatitis C virus (HCV) infection, Int. J. Med. Sci. 3 (2006) 47–52.
[2] F. Penin, J. Dubuisson, F.A. Rey, D. Moradpour, J.M. Pawlotsky, Structural biology of hepatitis C virus, Hepatology 39 (2004) 5–19.
[3] S.L. Tan, A. Pause, Y. Shi, N. Sonenberg, Hepatitis C therapeutics: current status and emerging strategies, Nat. Rev., Drug Discov. 1 (2002) 867–881.
[4] V.K. Wong, C. Cheong-Lee, J.A. Ford, E.M. Yoshida, Acute sensorineural hearing loss associated with peginterferon and ribavirin combination therapy during hepatitis C treatment: outcome after resumption of therapy, World J. Gastroenterol. 11 (2005) 5392–5393.
[5] K.E. Reed, C.M. Rice, Overview of hepatitis C virus genome structure, polyprotein processing, and protein properties, Curr. Top. Microbiol. Immunol. 242 (2000) 55–84.
[6] C. Vauloup-Fellous, V. Pene, J. Garaud-Aunis, F. Harper, S. Bardin, Y. Suire, E. Pichard, A. Schmitt, P. Sogni, G. Pierron, P. Briand, A.R. Rosenberg, Signal peptide peptidase-catalyzed cleavage of hepatitis C virus core protein is dispensable for virus budding but destabilizes the viral capsid, J. Biol. Chem. 281 (2006) 27679–27692.
[7] D. Lavillette, B. Bartosch, D. Nourrisson, G. Verney, F.L. Cosset, F. Penin, E.I. Pecheur, Hepatitis C virus glycoproteins mediate low pH-dependent membrane fusion with liposomes, J. Biol. Chem. 281 (2006) 3909–3917.
[8] B. Pozzetto, T. Bourlet, F. Grattard, L. Bonnevial, Structure, genomic organization, replication and variability of hepatitis C virus, Nephrol. Dial. Transplant. 11 (Suppl 4) (1996) 2–5.
[9] B. Bartosch, J. Dubuisson, F.L. Cosset, Infectious hepatitis C virus pseudo-particles containing functional E1–E2 envelope protein complexes, J. Exp. Med. 197 (2003) 633–642.
[10] A. Op De Beeck, R. Montserret, S. Duvet, L. Cocquerel, R. Cacan, B. Barberot, M. Le Maire, F. Penin, J. Dubuisson, The transmembrane domains of hepatitis C virus envelope glycoproteins E1 and E2 play a major role in heterodimerization, J. Biol. Chem. 275 (2000) 31428–31437.

[11] D. Lavillette, E.I. Pecheur, P. Donot, J. Fresquet, J. Molle, R. Corbau, M. Dreux, F. Penin, F.L. Cosset, Characterization of fusion determinants points to the involvement of three discrete regions of both E1 and E2 glycoproteins in the membrane fusion process of hepatitis C virus, J. Virol. 81 (2007) 8752–8765.

[12] R.F. Garry, S. Dash, Proteomics computational analyses suggest that hepatitis C virus E1 and pestivirus E2 envelope glycoproteins are truncated class II fusion proteins, Virology 307 (2003) 255–265.

[13] T.S. Jardetzky, R.A. Lamb, Virology: a class act, Nature 427 (2004) 307–308.

[14] B. Bartosch, F.L. Cosset, Cell entry of hepatitis C virus, Virology 348 (2006) 1–12.

[15] A.T. Yagnik, A. Lahm, A. Meola, R.M. Roccasecca, B.B. Ercole, A. Nicosia, A. Tramontano, A model for the hepatitis C virus envelope glycoprotein E2, Proteins 40 (2000) 355–366.

[16] R. Roccasecca, H. Ansuini, A. Vitelli, A. Meola, E. Scarselli, S. Acali, M. Pezzanera, B.B. Ercole, J. McKeating, A. Yagnik, A. Lahm, A. Tramontano, R. Cortese, A. Nicosia, Binding of the hepatitis C virus E2 glycoprotein to CD81 is strain specific and is modulated by a complex interplay between hypervariable regions 1 and 2, J. Virol. 77 (2003) 1856–1867.

[17] A.J. Perez-Berna, J. Guillen, M.R. Moreno, A. Bernabeu, G. Pabst, P. Laggner, J. Villalain, Identification of the membrane-active regions of hepatitis C virus p7 protein: biophysical characterization of the loop region, J. Biol. Chem. 283 (2008) 8089–8101.

[18] A.J. Perez-Berna, A.S. Veiga, M.A. Castanho, J. Villalain, Hepatitis C virus core protein binding to lipid membranes: the role of domains 1 and 2, J. Viral Hepatitis 15 (2008) 346–356.

[19] A.J. Perez-Berna, M.R. Moreno, J. Guillen, A. Bernabeu, J. Villalain, The membrane-active regions of the hepatitis C virus E1 and E2 envelope glycoproteins, Biochemistry 45 (2006) 3755–3768.

[20] L.J. Earp, S.E. Delos, H.E. Park, J.M. White, The many mechanisms of viral membrane fusion proteins, Curr. Top. Microbiol. Immunol. 285 (2005) 25–66.

[21] S.G. Peisajovich, Y. Shai, Viral fusion proteins: multiple regions contribute to membrane fusion, Biochim. Biophys. Acta 1614 (2003) 122–129.

[22] R.M. Epand, Fusion peptides and the mechanism of viral fusion, Biochim. Biophys. Acta 1614 (2003) 116–121.

[23] Y.P. Zhang, R.N. Lewis, R.S. Hodges, R.N. McElhaney, FTIR spectroscopic studies of the conformation and amide hydrogen exchange of a peptide model of the hydrophobic transmembrane alpha-helices of membrane proteins, Biochemistry 31 (1992) 11572–11578.

[24] L.D. Mayer, M.J. Hope, P.R. Cullis, Vesicles of variable sizes produced by a rapid extrusion procedure, Biochim. Biophys. Acta 858 (1986) 161–168.

[25] C.S.F. Böttcher, C.M. Van Gent, C. Fries, A rapid and sensitive sub-micro phosphorus determination, Anal. Chim. Acta 1061 (1961) 203–204.

[26] H. Edelhoch, Spectroscopic determination of tryptophan and tyrosine in proteins, Biochemistry 6 (1967) 1948–1954.

[27] D.K. Struck, D. Hoekstra, R.E. Pagano, Use of resonance energy transfer to monitor membrane fusion, Biochemistry 20 (1981) 4093–4099.

[28] M.R. Moreno, J. Guillen, A.J. Perez-Berna, D. Amoros, A.I. Gomez, A. Bernabeu, J. Villalain, Characterization of the interaction of two peptides from the N terminus of the NHR domain of HIV-1 gp41 with phospholipid membranes, Biochemistry 46 (2007) 10572–10584.

[29] B. Sainz Jr., J.M. Rausch, W.R. Gallaher, R.F. Garry, W.C. Wimley, Identification and characterization of the putative fusion peptide of the severe acute respiratory syndrome-associated coronavirus spike protein, J. Virol. 79 (2005) 7195–7206.

[30] M.R. Eftink, C.A. Ghiron, Exposure of tryptophanyl residues and protein dynamics, Biochemistry 16 (1977) 5546–5551.

[31] A.J. Perez-Berna, J. Guillen, M.R. Moreno, A.I. Gomez-Sanchez, G. Pabst, P. Laggner, J. Villalain, Interaction of the most membranotropic region of the HCV E2 envelope glycoprotein with membranes. Biophysical characterization, Biophys. J. 94 (12) (2008) 4737–4750.

[32] J. Wall, F. Ayoub, P. O'Shea, Interactions of macromolecules with the mammalian cell surface, J. Cell Sci. 108 (Pt 7) (1995) 2673–2682.

[33] E. Gross, R.S. Bedlack Jr., L.M. Loew, Dual-wavelength ratiometric fluorescence measurement of the membrane dipole potential, Biophys. J. 67 (1994) 208–216.

[34] M.F. Vitha, R.J. Clarke, Comparison of excitation and emission ratiometric fluorescence methods for quantifying the membrane dipole potential, Biochim. Biophys. Acta 1768 (2007) 107–114.

[35] A.S. Veiga, N.C. Santos, L.M. Loura, A. Fedorov, M.A. Castanho, HIV fusion inhibitor peptide T-1249 is able to insert or adsorb to lipidic bilayers. Putative correlation with improved efficiency, J. Am. Chem. Soc. 126 (2004) 14758–14763.

[36] P. Laggner, X-ray diffraction on biomembranes with emphasis on lipid moiety, Subcell. Biochem. 23 (1994) 451–491.

[37] G. Pabst, Global properties of biomimetic membranes: perspectives on molecular features, Biophys. Rev. Lett. 1 (2006) 57–84.

[38] L.M. Contreras, F.J. Aranda, F. Gavilanes, J.M. Gonzalez-Ros, J. Villalain, Structure and interaction with membrane model systems of a peptide derived from the major epitope region of HIV protein gp41: implications on viral fusion mechanism, Biochemistry 40 (2001) 3196–3207.

[39] D.M. Engelman, T.A. Steitz, A. Goldman, Identifying nonpolar transbilayer helices in amino acid sequences of membrane proteins, Annu. Rev. Biophys. Biophys. Chem. 15 (1986) 321–353.

[40] W.C. Wimley, S.H. White, Experimentally determined hydrophobicity scale for proteins at membrane interfaces, Nat. Struct. Biol. 3 (1996) 842–848.

[41] S.H. White, W.C. Wimley, Hydrophobic interactions of peptides with membrane interfaces, Biochim. Biophys. Acta 1376 (1998) 339–352.

[42] M.R. Moreno, M. Giudici, J. Villalain, The membranotropic regions of the endo and ecto domains of HIV gp41 envelope glycoprotein, Biochim. Biophys. Acta 1758 (2006) 111–123.

[43] H.E. Drummer, P. Poumbourios, Hepatitis C virus glycoprotein E2 contains a membrane-proximal heptad repeat sequence that is essential for E1E2 glycoprotein heterodimerization and viral entry, J. Biol. Chem. 279 (2004) 30066–30072.

[44] R. Pascual, M. Contreras, A. Fedorov, M. Prieto, J. Villalain, Interaction of a peptide derived from the N-heptad repeat region of gp41 Env ectodomain with model membranes. Modulation of phospholipid phase behavior, Biochemistry 44 (2005) 14275–14288.

[45] J.L. Nieva, F.M. Goni, A. Alonso, Liposome fusion catalytically induced by phospholipase C, Biochemistry 28 (1989) 7364–7367.

[46] N.C. Santos, M. Prieto, M.A. Castanho, Interaction of the major epitope region of HIV protein gp41 with membrane model systems. A fluorescence spectroscopy study, Biochemistry 37 (1998) 8674–8682.

[47] R. Pascual, M.R. Moreno, J. Villalain, A peptide pertaining to the loop segment of human immunodeficiency virus gp41 binds and interacts with model biomembranes: implications for the fusion mechanism, J. Virol. 79 (2005) 5142–5152.

[48] J. Wall, C.A. Golding, M. Van Veen, P. O'Shea, The use of fluoresceinphosphatidylethanolamine (FPE) as a real-time probe for peptide-membrane interactions, Mol. Membr. Biol. 12 (1995) 183–192.

[49] N. Fuller, C.R. Benatti, R.P. Rand, Curvature and bending constants for phosphatidylserine-containing membranes, Biophys. J. 85 (2003) 1667–1674.

[50] S. Chattopadhyay, P. Sun, P. Wang, B. Abonyo, N.L. Cross, L. Liu, Fusion of lamellar body with plasma membrane is driven by the dual action of annexin II tetramer and arachidonic acid, J. Biol. Chem. 278 (2003) 39675–39683.

[51] P. Meers, S. Ali, R. Erukulla, A.S. Janoff, Novel inner monolayer fusion assays reveal differential monolayer mixing associated with cation-dependent membrane fusion, Biochim. Biophys. Acta 1467 (2000) 227–243.

[52] A. Ahn, D.L. Gibbons, M. Kielian, The fusion peptide of Semliki Forest virus associates with sterol-rich membrane domains, J. Virol. 76 (2002) 3267–3275.

[53] D. Lavillette, A.W. Tarr, C. Voisset, P. Donot, B. Bartosch, C. Bain, A.H. Patel, J. Dubuisson, J.K. Ball, F.L. Cosset, Characterization of host-range and cell entry properties of the major genotypes and subtypes of hepatitis C virus, Hepatology 41 (2005) 265–274.

[54] R.F. de Almeida, A. Fedorov, M. Prieto, Sphingomyelin/phosphatidylcholine/cholesterol phase diagram: boundaries and composition of lipid rafts, Biophys. J. 85 (2003) 2406–2416.

[55] J.A. Killian, B. de Kruijff, The influence of proteins and peptides on the phase properties of lipids, Chem. Phys. Lipids 40 (1986) 259–284.

[56] M. Kielian, F.A. Rey, Virus membrane-fusion proteins: more than one way to make a hairpin, Nat. Rev., Microbiol. 4 (2006) 67–76.

[57] D.J. Schibli, W. Weissenhorn, Class I and class II viral fusion protein structures reveal similar principles in membrane fusion, Mol. Membr. Biol. 21 (2004) 361–371.

[58] S.A. Gallo, C.M. Finnegan, M. Viard, Y. Raviv, A. Dimitrov, S.S. Rawat, A. Puri, S. Durell, R. Blumenthal, The HIV Env-mediated fusion reaction, Biochim. Biophys. Acta 1614 (2003) 36–50.

[59] M. Kielian, I.I. Class, Virus membrane fusion proteins, Virology 344 (2006) 38–47.

[60] Y. Ciczora, N. Callens, F. Penin, E.I. Pecheur, J. Dubuisson, Transmembrane domains of hepatitis C virus envelope glycoproteins: residues involved in E1E2 heterodimerization and involvement of these domains in virus entry, J. Virol. 81 (2007) 2372–2381.

[61] Y. Ciczora, N. Callens, C. Montpellier, B. Bartosch, F.L. Cosset, A. Op de Beeck, J. Dubuisson, Contribution of the charged residues of hepatitis C virus glycoprotein E2 transmembrane domain to the functions of the E1E2 heterodimer, J. Gen. Virol. 86 (2005) 2793–2798.

[62] Z.Y. Keck, A. Op De Beeck, K.G. Hadlock, J. Xia, T.K. Li, J. Dubuisson, S.K. Foung, Hepatitis C virus E2 has three immunogenic domains containing conformational epitopes with distinct properties and biological functions, J. Virol. 78 (2004) 9224–9232.

[63] M. Brazzoli, A. Helenius, S.K. Foung, M. Houghton, S. Abrignani, M. Merola, Folding and dimerization of hepatitis C virus E1 and E2 glycoproteins in stably transfected CHO cells, Virology 332 (2005) 438–453.

[64] G. Pabst, S. Danner, R. Podgornik, J. Katsaras, Entropy-driven softening of fluid lipid bilayers by alamethicin, Langmuir 23 (2007) 11705–11711.

[65] G. Pabst, S.L. Grage, S. Danner-Pongratz, W. Jing, A.S. Ulrich, A. Watts, K. Lohner, A. Hickel, Membrane thickening by the antimicrobial peptide PGLa, Biophys. J. 95 (2008) 5779–5788.

[66] H.W. Huang, Molecular mechanism of antimicrobial peptides: the origin of cooperativity, Biochim. Biophys. Acta 1758 (2006) 1292–1302.

[67] S. Tristram-Nagle, J.F. Nagle, HIV-1 fusion peptide decreases bending energy and promotes curved fusion intermediates, Biophys. J. 93 (2007) 2048–2055.

[68] G. Pabst, J. Katsaras, V.A. Raghunathan, Enhancement of steric repulsion with temperature in oriented lipid multilayers, Phys. Rev. Lett. 88 (2002) 128101.

[69] B. Pozo-Navas, V.A. Raghunathan, J. Katsaras, M. Rappolt, K. Lohner, G. Pabst, Discontinuous unbinding of lipid multibilayers, Phys. Rev. Lett. 91 (2003) 028101.

[70] A.S. Dimitrov, X. Xiao, D.S. Dimitrov, R. Blumenthal, Early intermediates in HIV-1 envelope glycoprotein-mediated fusion triggered by CD4 and co-receptor complexes, J. Biol. Chem. 276 (2001) 30335–30341.

[71] J. Guillen, A.J. Perez-Berna, M.R. Moreno, J. Villalain, Identification of the membrane-active regions of the severe acute respiratory syndrome coronavirus spike membrane glycoprotein using a 16/18-mer peptide scan: implications for the viral fusion mechanism, J. Virol. 79 (2005) 1743–1752.